JOURNAL OF MATERIALS SCIENCE **36** (2001) 4681–4686

# Deformation and energy absorption of wood cell walls with different nanostructure under tensile loading

A. REITERER*
*Institute of Meteorology and Physics & Christian Doppler Laboratory for Fundamentals of Wood Machining, University of Agricultural Sciences Vienna, Türkenschanzstraße 18, A-1180 Vienna, Austria*
*E-mail: alexander.reiterer@fff.co.at*

H. LICHTENEGGER, P. FRATZL
*Erich Schmid Institute for Material Science of the Austrian Academy of Sciences & Metal Physics Institute, University Leoben, Jahnstraße 12, A-8700 Leoben, Austria*

S. E. STANZL-TSCHEGG
*Institute of Meteorology and Physics & Christian Doppler Laboratory for Fundamentals of Wood Machining, University of Agricultural Sciences Vienna, Türkenschanzstraße 18, A-1180 Vienna, Austria*

The nanostructure of the S2 cell wall layer in tracheids of Picea abies (Norwegian spruce), in particular the cellulose microfibril angle, has been shown to control not only the stiffness but also the extensibility of wood within a wide range. In order to further elucidate this effect, the deformation of wood under tensile load parallel to the longitudinal cell axis was studied in a contact-free way using a video extensometer. The combination of these measurements with small-angle X-ray scattering on the same microtome sections allowed us to establish a direct relationship between the microfibril angle and deformation behaviour. The microfibril angle was shown to influence not only the extensibility in longitudinal direction but also the deformation perpendicular to the applied load. Moreover, the results showed that the energy absorption capacity is higher for specimens with larger microfibril angle. SEM pictures of the fractured samples indicated clearly the differences in the fracture process as the fracture zones of samples with low microfibril angle were smooth and the fracture zones of samples with high microfibril angle were heavily torn and deformed indicating a more ductile behaviour. 

## 1. Introduction

The complicated hierarchical and cellular structure of wood is well known to provide excellent mechanical properties, in particular with regard to their low weight [1]. Softwoods like *Picea abies* (Norwegian spruce) are most appropriate for investigating the influence of the cell wall architecture on mechanical properties, since about 95% of the wood cells are tracheids and the influence of different cell morphologies can be neglected. The wood cell wall consists of stiff, partly cristalline elementary cellulose fibrils embedded in an amorphous hemicellulose-lignin matrix, running fairly parallel to one another in the major part of the cell wall, the S2 layer. In tracheids of *Picea abies* the S2 layer represents up to 75–85% of the cell wall [2] and therefore its internal structure plays a keyrole in determining the mechanical properties, especially under load parallel to the grain. The angle of the elementary cellulose fibrils with respect to the longitudinal cell axis, the microfibril angle, was found to be a crucial factor in determining mechanical properties like stiffness [3, 4], extensibility [4] and shrinkage [5].

In the present paper small-angle X-ray scattering (SAXS) and tensile tests parallel to the grain were combined to investigate the influence of the microfibril angle on the deformation behaviour parallel and perpendicular to the applied load as well as on the energy absorption capacity. Both methods were performed on the same samples to obtain a direct relationship between nanostructure and mechanics.

## 2. Materials and methods

### 2.1. Mechanical measurements

Normal samples of spruce wood (*Picea abies*), were collected from the stem, the upper and lower side of a branch, respectively. Tangential slices were cut out of earlywood and latewood of the stem and two annual

* *Present address*: Austrian Industrial Research Promotion Fund, Kärtnerstr. 21-23, A-1015 Vienna, Austria.

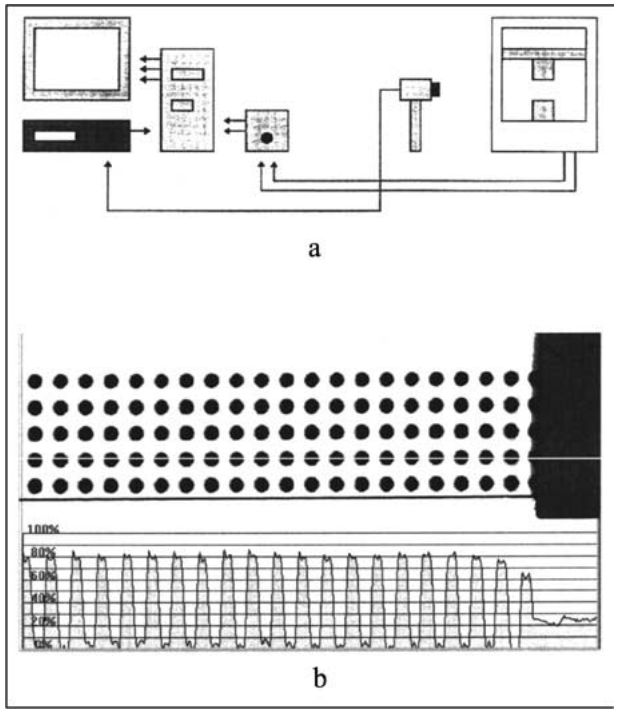


*Figure 1* (a) Videoextensometer dataflow diagramm; from the right to the left: universal testing machine, CCD-camera, VCO, computer, videorecoder; (b) Specimen with brightness variation along the white line.

rings of the lower and upper side of the branch. The ends of the samples were pasted to a 1 mm thick foil to prevent damaging of the samples when gripped in the jaws of a standard testing machine. Tensile tests were carried out with a constant cross-head speed of 0.2 mm/min using a standard material testing machine (QTS 10). The moisture content of the samples was kept above the fibre saturation point, where the influence of the moisture content on mechanical properties is insignificant [6].

In order to determine the strain in two dimensions (longitudinal and tangential) in a contact free way an optical system (videoextensometer) was used. A regular array of black points was plotted on the sample surface and images of the sample were recorded subsequently by a CCD camera during deformation (see Fig. 1). The point displacements gave information on the surface displacements, as described in [7]. In this paper the strains in longitudinal and tangential direction $\varepsilon_l$ and $\varepsilon_q$ were evaluated simultaneously.

## 2.2. Structural measurements

In order to obtain a correlation between deformation of the samples and their structure, the same samples stressed in the tensile tests were used for investigation by small-angle X-ray scattering. Without any further treatment, they were encapsulated in plastic foils in order to prevent drying in the vacuum chamber of the X-ray equipment (Bruker AXS). They were exposed to Cu $K_\alpha$ radiation and SAXS patterns were obtained by a two-dimensional position sensitive detector with a typical time of 45 minutes per scattering pattern to provide sufficient counting statistics.

The method of SAXS is sensitive to the electron density contrast between the elementary cellulose fibrils

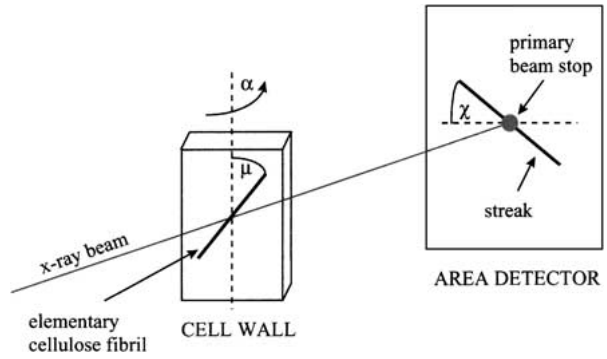


*Figure 2* Scattering geometry showing an elementary cellulose fibril in the cell wall and the streak produced on the area detector. The orientation of the streak $\chi$ can be used to determine the microfibril angle $\mu$.

and the hemicellulose/lignin matrix. The scattering pattern can be used to evaluate the microfibril angle, as described in detail for example in [4, 8–11]. In Fig. 2 only the principle is sketched: A long, thin cylinder such as a cellulose fibril produces a narrow streak of high intensity perpendicular to the fibril on a two-dimensional detector. The orientation $\chi$ of the streak can thus be used to determine the orientation $\mu$ of the fibril.

## 3. Results

The structural investigations showed that for wood from the stem two different microfibril angles were found. The microfibril angle of earlywood samples and of latewood samples of annual rings near the bark was found to be approximately 5°, indicating an orientation of the cellulose fibrils roughly parallel to the longitudinal direction of the wood cell. In latewood samples from a lot of annual rings (all from the mature zone) a microfibril angle of approximately 20° was found. In the branch higher microfibril angles were found, reaching 26° on the upper and 50° on the lower side.

The longitudinal strain $\varepsilon_l$ and the tangential strain $\varepsilon_q$ are shown as a function of the microfibril angle in Fig. 3a. Each datapoint is a mean value of 10–15 specimens. The error bars indicate the standard deviations.

The maximum longitudinal strain $\varepsilon_l$ increased from 0.5% to 11% as the microfibril angle changed from about 5° to 50°. This is a confirmation of earlier findings from conventional tensile tests [4]. However, here, the use of videoextensometry yields a much higher accuracy, especially for very low strains, as the achieved resolution is in the range of 4 $\mu$m. The enormous increase of extensibility with increasing microfibril angle is mainly due to irreversible deformation as can be seen in Fig. 3b where the ratio of irreversible longitudinal strain $\varepsilon_{l,i}$ to the total longitudinal strain $\varepsilon_l$ is depicted.

Most interesting, not only the longitudinal strain but also the tangential strain is a function of the microfibril angle as can be seen in Fig. 3a. The absolute value of the tangential strain $\varepsilon_q$ increased as the microfibril angle increased from 5° to 20° and after reaching a maximum at 27° the absolute value decreased for the specimens with a microfibril angle of 50°.

The total Poisson ratio

$$\nu_{\text{total}} = -\varepsilon_q/\varepsilon_l \qquad (1)$$

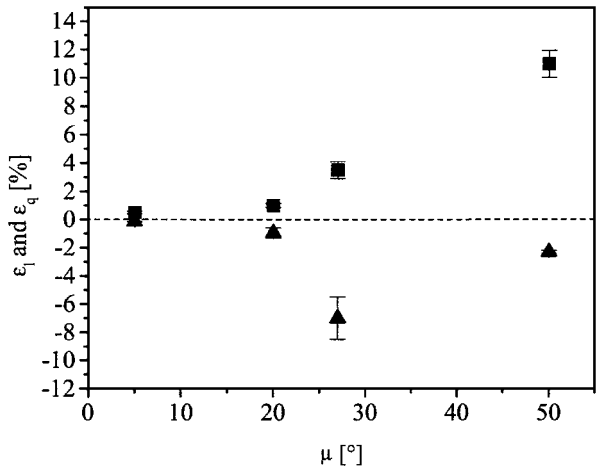


(a)

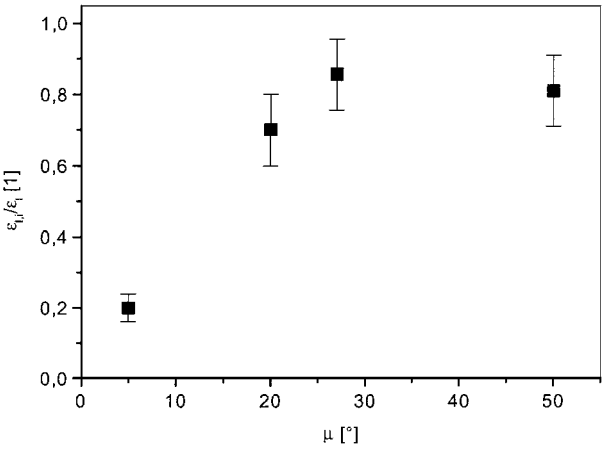


(b)

*Figure 3* (a) Maximum longitudinal strain $\varepsilon_l$ (squares) and maximum tangential strain $\varepsilon_t$ (triangles) versus the microfibril angle $\mu$. (b) Ratio of the irreversibel part of the longitudinal strain $\varepsilon_{l,i}$ to the maximum longitudinal strain $\varepsilon_l$ versus the microfibril angle $\mu$.

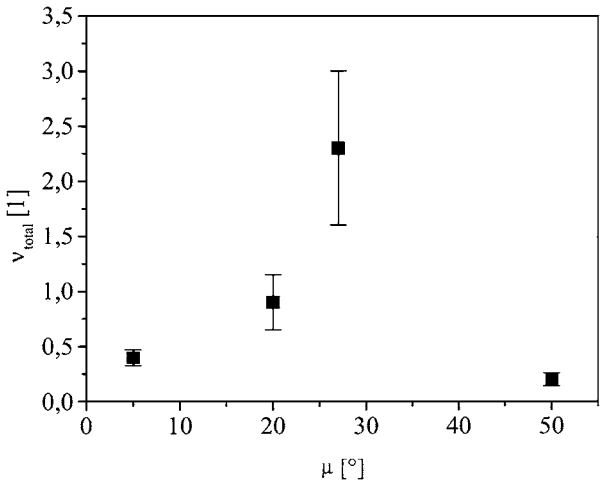


*Figure 4* Total Poisson ratio $\nu_{total}$ versus the microfibril angle $\mu$.

considering both, the elastic and the irreversible part of the tangential and longitudinal deformation, reached a maximum of 2.2 at a microfibril angle of 27° (Fig. 4).

Tensile strength $\sigma_{max}$ as well the proportional limit $\sigma_p$ decreases with increasing MFA as can be seen in Fig. 5. The stresses were normalized by the ratio of cell wall density to the density of the sample. The tensile strength

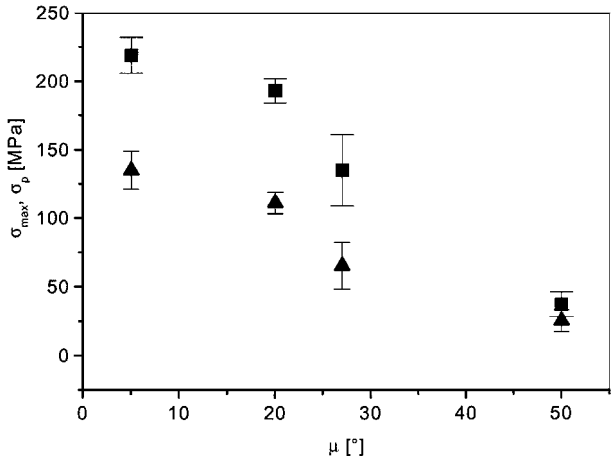


*Figure 5* Tensile strength $\sigma_{max}$ (squares) and proportional limit $\sigma_p$ (triangles) versus the microfibril angle $\mu$.

decreased from 220 MPa at a microfibril angle of 5° to approximately 35 MPa at an angle of 50° whereas the proportional limit decreased from 135 MPa to 25 MPa.

In order to characterize the energy absorbing capacity the work of fracture $W_{total}$ of the investigated samples was evaluated from the stress-strain curves as an energy per volume according to

$$\begin{aligned} W_{total} &= \int_0^{\varepsilon_{l,el}} \sigma \, d\varepsilon + \int_{\varepsilon l,el}^{\varepsilon_l} \sigma(\varepsilon) \, d\varepsilon \\ &= \frac{1}{2}\sigma_p \varepsilon_{l,el} + \int_{\varepsilon_{l,el}}^{\varepsilon_l} \sigma(\varepsilon) \, d\varepsilon \\ &= W_{el} + W_{irr}. \end{aligned} \tag{2}$$

The first part, $W_{el}$, is the energy absorption due to elastic deformations, $\sigma_p$ is the proportional limit and $\varepsilon_{l,el}$ the elastic part of the longitudinal strain. The second part, $W_{irr}$, is due to the irreversible deformations and $\varepsilon_l$ is the total longitudinal strain.

The work of fracture is plotted versus the microfibril angle in Fig. 6a. As can be seen the absorbed energy during tensile loading increased from small microfibril angles up to angles around 30–40° approximately by a factor 6. For higher microfibril angles the energy absorption is mainly due to inelastic deformation. The fraction of absorbed energy due to elastic deformation is only approximately 10% (see Fig. 6b). In 1974, Gordon and Jeronimidis [12] used cylindrical tubes with walls of helically wound glass or carbon fibers to simulate the structure of wood. They found that the work of fracture was highest at indermediate winding angles of approximately 15°.

The topology of the fracture zones of the tested specimen reflects the different energy absorbing capacity. In Fig. 7 a fracture zone of a wood specimen with a microfibril angle of about 5° is shown. The fracture surface is smooth and there are only few cell wall fragments visible indicating a brittle fracture process. Quite in contrast the fracture zone of wood specimens with a microfibril angle of 50° (see Fig. 7b) shows a rough surface with highly deformed tracheids. Torn cell wall fragments spiraling out of the fractured tracheids indicate the ductile character of the fracture process.

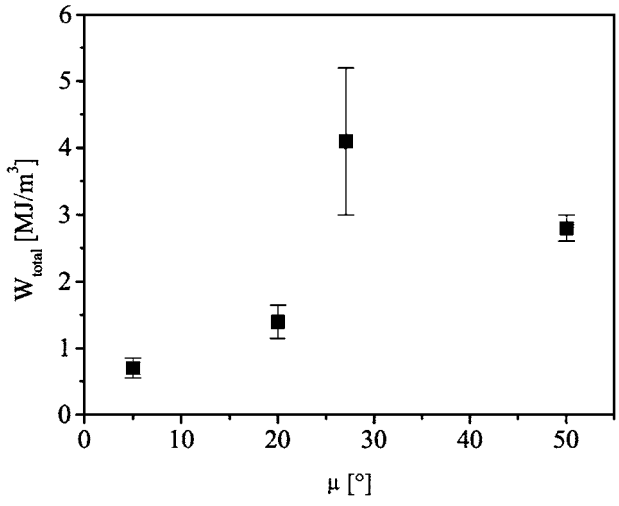


(a)

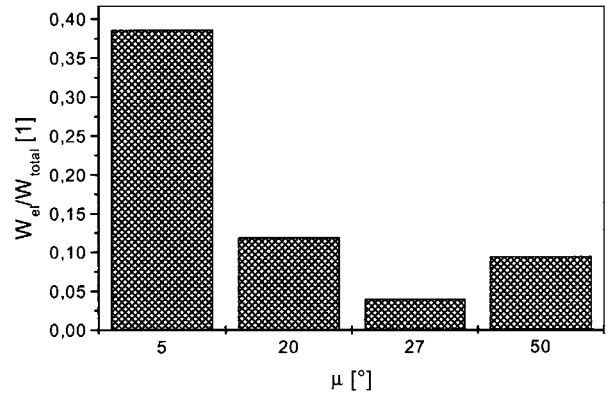


(b)

*Figure 6* (a) Total work of fracture $W_{\text{total}}$ versus the microfibril angle $\mu$. (b) Ratio of the part of the work of fracture due to elastic deformations $W_{\text{er}}$ to the total work of fracture $W_{\text{total}}$ versus the microfibril angle $\mu$.

## 4. Discussion

The increase of the longitudinal fracture strain under tension with increasing microfibril angle was found also for single wood fibers (see for example [13, 14]). Since a tube like construction with spirally wound fibers could be unstable under a process called, "tension buckling" [15] it was concluded that the cell walls buckle into the lumen in such a way that high longitudinal extensions are possible [12, 13, 16]. Later, this explanation was rejected [14], since tension buckling should primarily be observed in thin-walled fibres. It was argued that wood cell walls are thick enough to withstand buckling.

It is generally recognized, however, that at higher microfibril angles the shear stress in the interfibrillar matrix rises. This could lead to large irreversible extension as the yield point of the matrix will be reached and flow will begin. This mechanism was discussed for single fibers by Page and El-Hosseiny [14]. Moreover Navi *et al.* [17] argued that in a thin wood specimen consisting of a small number of individual wood fibers the matrix should be damaged under tensile load in zones where the microfibril angles are larger. Actually, small-angle X-ray scattering results showed that there is not a single microfibril angle but a certain distribution of microfibril angles about a mean value. Typical distribution widths of approximately 8° have been found for earlywood and latewood of spruce [10]. Recently, Perez *et al.* [18] showed on single wood fibers that such local matrix damage could also produce a hinge along the fibre allowing one part of the fibre to twist against the other part. In a wood specimen there will be an interaction between adjacent cell walls leading to shear restraint as adjacent wall sections would have to undergo displacements in opposite directions [19]. However, tensile loading of a wood specimen could lead to lateral separation along the middle lamela which consits mainly of matrix substances (lignin and hemicellulose). This is likeley in the immediate neighbourhood of the fracture zone at the begin of the irreversibility and would enable the cells in that region to undergo further large irreversible deformations due to the above described mechanism.

This large deformation should result in a local decrease of the microfibril angle [18]. No direct observation of a decrease could be shown up to now due to the experimental difficulties for such an in-situ experiment. However, Spatz *et al.* [20], showed in cyclic loading-unloading tensile experiments on 200 $\mu$m thick samples of *Aristolochia macrophylla* a slight decrease of the microfibril angle from 22° to 18°, measured by polarization microscopy, after loading-unloading. This result could point to such a mechanism.

The total Poisson ratio obtained in our experiment varied from 0.2 to 2.2. In isotropic materials a Poisson ratio $>1$ would clearly indicate inelastic deformation. In a technical composite materials such as symmetric laminates with very different mechanical properties of matrix and fiber (see for example [21]), however, purely elastic Poisson ratios $>1$ can be observed. In such materials, extensional shear-coupling can lead to a maximum of the elastic Possion ratio for a winding angle of the reinforcing fibers of approximately 30°. Considering the fact that in two neighbourhood cell walls the S2 layers form a symmetric laminate in a simple approximation [22], the total Poisson ratio of the wood cell walls may be unterstood qualitatively. However, the wood cell wall is a real nanocomposite. In this investigation a distinction between an elastic and an irreversible part of the deformation perpendicular to the applied load was not possible.

Recently, the course of microfibril angles versus the life span of trees was interpreted in a view of a mechanical optimization due to different loading situations acting on a tree [10]. In this interpretation loading by wind and gravitational forces demand high moduli of elasticity and high strength values. Stiffness decreases as MFA increases [3, 4]. Tensile strength as well as the proportional limit decreases too with increasing MFA as can be seen in Fig. 5. A third loading case, bending up to a critical angle, demands for a high extensibility. The extensibility increases with increasing MFA ([4] and Fig. 3). All these quantities determine in a complex interaction the total absorbed energy during tensile loading due to the needs of various parts under different kinds of loading.

In order to quantify the relative merit in providing a combination of strength on the one hand and energy absorption capacity on the other the following relative

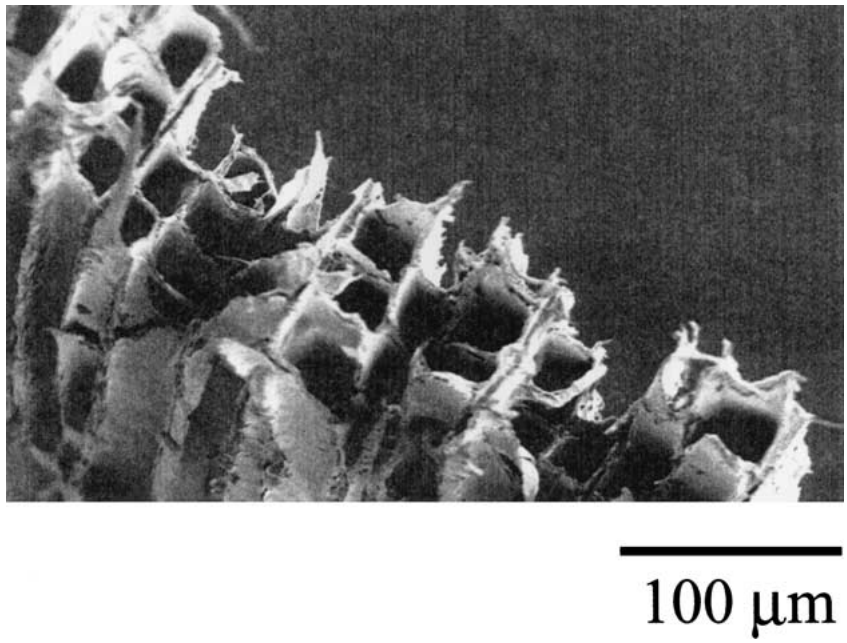


(a)

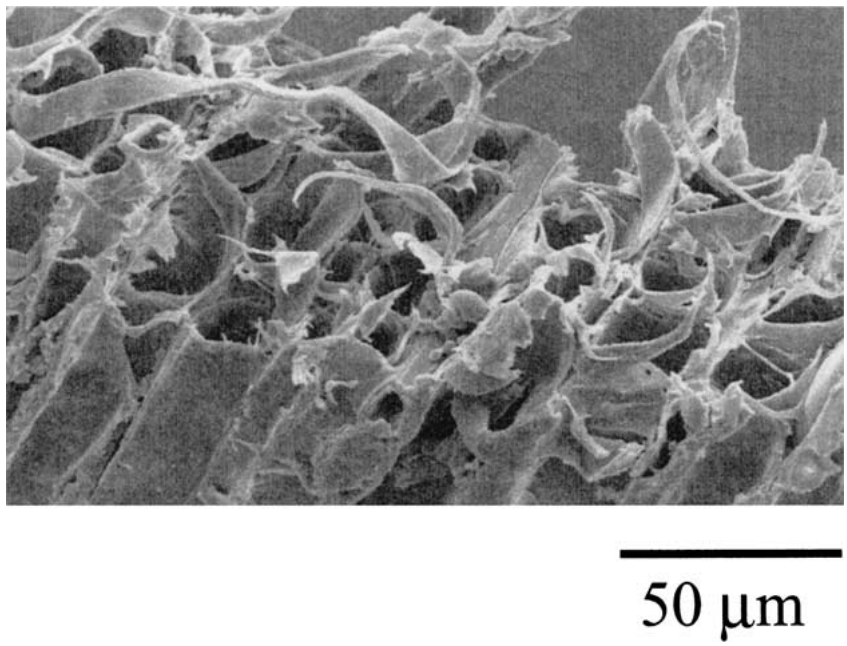


(b)

*Figure 7* (a) SEM picture of the fracture zone of a specimen with a microfibril angle of about 5°. The fracture surface is smooth; (b) SEM picture of the fracture zone of a specimen with a microfibril angle of about 50°. The fracture surface is heavily deformed and torn cell wall fragments are spiraling out of the tracheids.

quantity according to [12], has been used:

$$A(\mu) = \frac{W_{\text{total}}(\mu)\sigma_{\max}(\mu)}{W_{\text{total}}(5^\circ)\sigma_{\max}(5^\circ)} \tag{3}$$

The product of the total work of fracture at a microfibril angle $\mu$, $W(\mu)$ and the tensile strength $\sigma_{\max}(\mu)$ is normalized with the product of the two parameters when the cellulose fibrils are oriented almost parallel to the longitudinal cell axis. In Fig. 8 $A(\mu)$ is plotted versus the microfibril angle. It can be seen that the best compromise between loss of strength and increase of energy absorbing capacity is obtained for the specimens with a microfibril angle of about 27°. Most interesting, this microfibril angle was found for the specimens of the upper part of the branch. The upper part is typically under tension load due to its own weight. Therefore, a certain tensile strength is necessary. On the other hand bending up to an critical angle, where for example snow glides off, demands for a high enough extensibility.

It should be marked that other anatomical features like cell wall diamter or cell size vary and that at the bottom of the branch compression wood is formed which is known to have less cellulose and more lignin than normal wood. These parameters might also influence the mechanical properties. Nevertheless our results show a distinct relationship between the microfibril angle and the deformation behaviour.

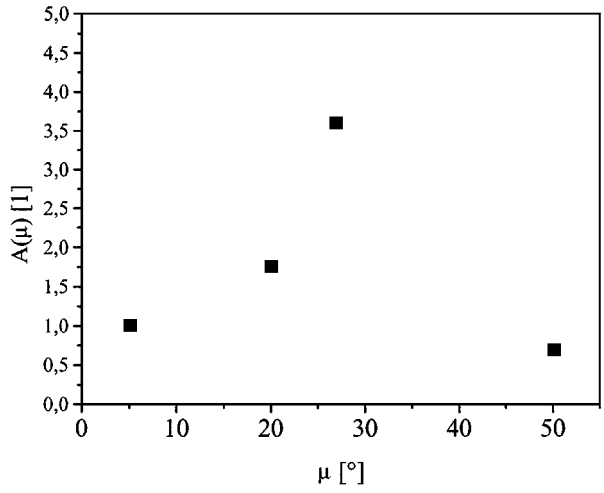


*Figure 8* Relative merit in providing a combination of strength and energy absorbing capacity $A(\mu)$ versus the microfibril angle.

## 5. Conclusions

In this paper tensile tests supported by videoextensometry and small-angle X-ray scattering were used to investigate the relationship between deformation and nanostructure of thin wood sections. The experimental results establish that there is not only a strong influence of the microfibril angle on the deformation parallel to an applied tensile load but also in the perpendicular direction. The determined total Poisson ratio is highest at intermediate microfibril angles. It was shown that higher microfibril angles provide much higher total work of fracture than lower ones. SEM pictures of the fracture zones showed a smooth fracture surface reflecting brittle fracture in the case of small MFAs and torn cell walls with cell wall fragments spiralling out of the tracheids in the case of large MFAs. The best compromise between a loss in strength and an increase in energy absorbing capacity was found for intermediate microfibril angles around 27°.

## References


1. M. F. ASHBY, *Acta Metall.* **37** (1984) 1273.
2. D. FENGEL and G. WEGENER, "Wood—Chemistry, Ultrastructure, Reactions" (De Gruyter, Berlin, New York, 1989).
3. I. D. CAVE, *Wood Sci. Technol.* **3** (1969) 40.
4. A. REITERER, H. LICHTENEGGER, S. TSCHEGG and P. FRATZL, *Phil. Mag. A* **79** (1999) 2173.
5. B. A. MEYLAN, *Wood Sci. Technol.* **6** (1972) 293.
6. J. M. DINWOODIE, "Wood—Nature's Cellular Polymeric Fibre-composite" (The Institute of Metals, 1989).
7. G. SINN, A. REITERER, S. E. STANZL-TSCHEGG and E. K. TSCHEGG, *Holz Roh-Werkstoff* **59** (2001) 177.
8. H. F. JAKOB, P. FRATZL and S. E. TSCHEGG, *J. Struct. Biol.* **113** (1994) 13.
9. H. LICHTENEGGER, A. REITERER, S. TSCHEGG and P. FRATZL, in "Microfibril Angle in Wood," edited by B. J. Butterfield (University of Canterbury, Christchurch, New Zealand, 1998) p. 140.
10. H. LICHTENEGGER, A. REITERER, S. TSCHEGG and P. FRATZL, *J. Struct. Biol.* **128** (1999) 257.
11. A. REITERER, H. F. JAKOB, S. TSCHEGG and P. FRATZL, *Wood Sci. Technol.* **32** (1998) 335.
12. J. E. GORDON and G. JERONIMIDIS, *Phil. Trans. R. Soc. Lond. A* **294** (1982) 545.
13. D. H. PAGE, F. EL-HOSSEINY and K. WINKLER, *Nature* **229** (1971) 252.
14. D. H. PAGE and F. EL-HOSSEINY, *J. Pulp Paper Sci.* **9** (1983) TR99.
15. N. J. PAGANO, J. C. HALPIN and J. W. WHITNEY, *J. Comp. Mat.* **2** (1968) 154.
16. J. E. GORDON and G. JERONIMIDIS, *Nature* **252** (1971) 116.
17. P. NAVI, P. K. RASTOGI, V. GRESSE and A. TOLOU, *Wood Sci. Technol.* **29** (1995) 411.
18. L. PEREZ, V. PITTET and P. NAVI, in Proc. Internat. Conf. Wood and Wood Fibre Composites, edited by S. Aicher (University of Stuttgart, 2000) p. 47.
19. A. P. SCHNIEWIND and J. D. BARRETT, *Wood Fiber* **1** (1969) 205.
20. H.-CH. SPATZ, L. KÖHLER and K. J. NIKLAS, *J. Exp. Bot.* **202** (1999) 3269.
21. ASM International, "Engineered Materials Handbook Volume 1: Composites" (ASM International Ohio, 1987).
22. J. BODIG and B. A. JAYNE, "Mechanics of Wood and Wood Composites" (Krieger Publishing Company, Florida, 1993).



*Received 28 August 2000*
*and accepted 13 April 2001*